

Global systematics of arc volcano position

Philip C. England¹ & Richard F. Katz¹

¹Department of Earth Sciences, Parks Road, Oxford OX1 3PR. UK.

This is an author-prepared copy of the final version of this paper. The published version is in Nature, v468, 700-704, doi:10.1038/nature09154

<http://www.nature.com/nature/journal/v468/n7325/full/nature09154.html>

Global systematics in the location of volcanic arcs above subduction zones^{1,2} are widely considered to be a clue to the melting processes that occur at depth, and the locations of the arcs have often been explained in terms of the release of hydrous fluids near the top of the subducting slab (e.g. ³⁻⁶). Grove *et al.*⁷ hypothesize that arc location is controlled by melting in the mantle at temperatures above the water-saturated upper-mantle solidus and below the upper limit of stability of the mineral chlorite (conditions defined as P, T_{melt} in their Fig 1b). Specifically, they argue that arc volcanism occurs directly above the shallowest point of the region in which mantle conditions satisfy the P, T_{melt} criterion. Grove *et al.*⁷ then use numerical models of subduction zones to predict arc location and its global systematics. They conclude that agreement between their calculated systematics of arc location and observations of real subduction zones^{2,8} validates their hypothesis (Grove *et al.*⁷, Figure 3). We show that this conclusion is undermined by two flaws: first, Grove *et al.*'s⁷ calculated arc locations are in error due to inadequate spatial resolution of their numerical models; second, the agreement that they find between predicted and observed systematics arises from a spurious correlation of calculated arc location with slab dip.

Before we address these two points in detail, however, a problem with the results presented by Grove *et al.*⁷ is evident. A characteristic feature of subduction-zone models⁹ is the narrow thermal boundary layer, sub-parallel to and just above the slab surface, which contains the temperature range of P, T_{melt} (~ 800 – 850°C). For all but the slowest convergence rates, this boundary layer begins close to the depth at which the slab is viscously coupled to the wedge. Hence one should expect the region enclosing P, T_{melt} to be a very thin, continuous layer above the slab, with its shallowest extent at an essentially constant depth. The results of Grove *et al.*⁷ (green points in Fig. 2) are inconsistent with this expectation, and raise the suspicion of an error in their calculation.

To locate their region of P, T_{melt} , Grove *et al.*⁷ determined which nodes of their 2.3×2.3 -km computational mesh lay within that $P - T$ range. Because those conditions occur within a boundary layer only a few kilometres thick that is inclined at an angle to the mesh, this procedure did not resolve the full extent of the P, T_{melt} region. To check their results, we calculated the temperature fields for subduction zones on a 1×1 -km grid, then resampled it to both 2.3 km and to 0.25 km resolution. This was done for a range of subduction parameters and for each calculation we determined the P, T_{melt} region and its shallowest point. We found that at 2.3-km resolution, the minimum depth of P, T_{melt} ranged between about 57 and 76 km, consistent with the range found by Grove *et al.*⁷. On the 0.25 km grid, however, the minimum depth was confined between 57 and 61 km (Figure 1a), consistent with expectations laid out in the preceding paragraph. At either resolution, the minimum depth of P, T_{melt} is independent of the slab dip and of the convergence rate.

Grove *et al.*⁷ compare their calculations with seismic studies, which show that the depth-to-slab beneath arcs varies between ~ 80 and ~ 150 kilometres^{2,8} and has a negative correlation with the descent speed of the slab (Figure 1b). The depth to the top of the slab predicted by Grove *et al.*'s⁷ hypothesis applied under our recalculations is ~ 60 – 75 km, independent of dip or convergence rate (Figure 1b), and thus is in disagreement with the observations.

The agreement between model and observations in Grove *et al.*⁷ is spurious, and is the result of their choice of variables. Figure 1c recreates their Figure 3, which shows the apparent consistency between model and observations, using our recalculated location of arcs. The sine of slab dip is plotted on the x -axis, and on the y -axis is the distance to the trench, which for all points (calculated and observed – Grove *et al.*⁷, Table 1) is taken as the depth-to-slab divided by the tangent of the dip. The presence of the sine of the dip on each axis ensures a spurious correlation; this is illustrated clearly in Figure 1c by the grey line that corresponds to a constant value of $D_{Slab} = 62$ km.

Thus there is no significance in the match between models and observations reported by Grove *et al.*⁷, and their conclusion that “the kinematic control on the location of mantle melting is primarily slab dip” (Grove *et al.*⁷, p. 696) is mistaken. A more informative conclusion to draw from their experiments is that the limits of chlorite stability (Grove *et al.* Figure 1b)⁷ cannot explain the global systematics in the depth to the slab beneath the sharply localized arc fronts. Indeed, this remark applies to any strongly temperature-dependent processes that takes place near the top of the slab, for the reasons laid out in this comment.

1. Tovish, A. & Schubert, G. Island arc curvature, velocity of convergence and angle of subduction. *Geophys. Res. Letts.* **5**, 329–332 (1978).
2. England, P., Engdahl, R. & Thatcher, W. Systematic variation in the depths of slabs beneath arc volcanoes. *Geophys. J. Int.* **156**, 377–408 (2004).
3. Gill, J. *Orogenic Andesites and Plate Tectonics* (Springer-Verlag, New York, 1981).
4. Tatsumi, Y. & Eggins, S. *Subduction Zone Magmatism* (Blackwell Science, Cambridge, MA, 1995).
5. Iwamori, H. Transportation of H₂O and melting in subduction zones. *Earth Plan. Sci. Lett.* **160**, 65–80 (1998).
6. Tatsumi, Y. The subduction factory: How it operates in the evolving Earth. *GSA Today* **15**, 4–10 (2005).
7. Grove, T., Till, C., Lev, E., Chatterjee, N. & Médard, E. Kinematic variables and water transport control the formation and location of arc volcanoes. *Nature* **459**, 694–697 (2009).
8. Syracuse, E. & Abers, G. Global compilation of variations in slab depth beneath arc volcanoes and implications. *Geochem. Geophys. Geosys.* **7**, 18.
9. van Keken, P. *et al.* A community benchmark for subduction zone modeling. *Phys. Earth Planet. In.* **171**, 187–197 (2008).

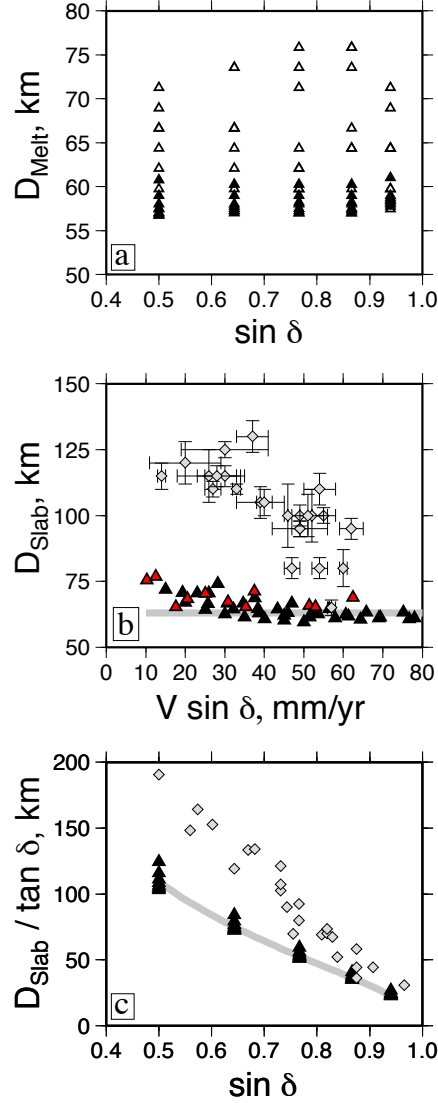


Figure 1: (a) Calculated depth D_{Melt} of the shallowest portion of the P, T_{melt} -based melting field (c.f. Figs. 1 and 2 of Grove *et al.*⁷). Calculations were carried out on a 1-km finite-volume mesh⁹, for dip δ of 30° to 70° in steps of 10° , and for convergence rate V from 30 to 100 mm/yr, in steps of 10mm/yr; these ranges include the parameters of the calculations of Grove *et al.*⁷. The points correspond to the minimum depths of melting calculated according to the hypothesis and methods of Grove *et al.*⁷ for 2.3×2.3 km resampled grid (open triangles) and for a 0.25×0.25 km resampled grid (filled triangles). (b) Diamonds show depth-to-slab determined seismologically²; filled triangles show the calculated depth of the slab D_{Slab} below the locus of shallowest melting, for the 0.25km resampled grid from panel (a). The red triangles correspond to the corrected upper limits of the P, T_{melt} region for the combinations of dip and convergence rate used by Grove *et al.*⁷ (T. Grove *et al.*, *pers. comm*). The grey line corresponds to a constant $D_{Slab} = 62$ km. (c) Points as for panel (b), plotted on an ordinate that is the horizontal distance between the trench and the arc (which is equal to $D_{Slab} / \tan \delta$). The grey line corresponds to $D_{Slab} = 62$ km and demonstrates the spurious correlation referred to in the text. This panel corresponds to the lower 200km of Grove *et al.*⁷, Figure 3.